Water Resources Research

RESEARCH ARTICLE
10.1029/2024WR039014

Decoupling Phytoplankton Biomass—Sediment Phosphorus Interaction Induced by Lower Incident Radiation Mainly Drives the Attenuation of Harmful Algal Blooms in Lake Taihu, China

Ting Pan[1,2], Justin Brookes[3], Chixiao Cui[1], Boqiang Qin[1,2,4], Kan Ding[1], Yunlin Zhang[1], and Guangwei Zhu[1]

[1]State Key Laboratory of Lake Science and Environment, Nanjing Institute of Geography and Limnology, Chinese Academy of Sciences, Nanjing, P. R. China, [2]College of Hydrology and Water Resources, Hohai University, Nanjing, P. R. China, [3]School of Biological Sciences, University of Adelaide, Adelaide, SA, Australia, [4]School of Geography & Ocean Science, Nanjing University, Nanjing, P. R. China

Key Points:

- The drivers behind the shift from high to low in algal biomass during 2016–2023 in Lake Taihu were explored using a process-based model
- Lower photosynthetically active radiation causes the decoupling of algal biomass-sediment phosphorus and decline of phytoplankton biomass
- Reducing external load is needed to weaken this algal biomass-sediment phosphorus feedback in eutrophic lakes

Supporting Information:

Supporting Information may be found in the online version of this article.

Correspondence to:

B. Qin,
qinbq@niglas.ac.cn

Citation:

Pan, T., Brookes, J., Cui, C., Qin, B., Ding, K., Zhang, Y., & Zhu, G. (2025). Decoupling phytoplankton biomass—Sediment phosphorus interaction induced by lower incident radiation mainly drives the attenuation of harmful algal blooms in Lake Taihu, China. *Water Resources Research*, *61*, e2024WR039014. https://doi.org/10.1029/2024WR039014

Received 23 SEP 2024
Accepted 27 MAY 2025

Author Contributions:

Conceptualization: Boqiang Qin
Data curation: Ting Pan
Formal analysis: Ting Pan
Funding acquisition: Chixiao Cui, Boqiang Qin
Investigation: Ting Pan
Methodology: Ting Pan, Boqiang Qin
Supervision: Boqiang Qin
Writing – original draft: Ting Pan
Writing – review & editing: Justin Brookes, Chixiao Cui, Boqiang Qin, Kan Ding, Yunlin Zhang, Guangwei Zhu

Abstract The occurrence, timing and development of algal blooms can be unpredictable under changing climatic conditions. Dramatic fluctuations in algal biomass patterns occurred in Lake Taihu, with a notable surge in blooms magnitude during 2016–2020 followed by a sudden decrease in algal biomass in the period of 2021–2023. The mechanisms underlying this variability are not well understood. Here, a process-based model was developed to quantify the drivers behind the transition from higher to lower algal biomass patterns. The lower spring photosynthetically active radiation (PAR) during 2021–2023 decreased algal photosynthesis and algal biomass. The subsequent weak phytoplankton–phosphorus (from the sediment) feedback, resulted in decreased phosphate concentration, which in turn further reduced algal biomass. This mechanism underscores the importance of understanding internal nutrient dynamics and the need for stricter measures to reduce external loads to weaken the internal feedback loop between sediment phosphorus release and algal bloom outbreaks, and further to mitigate the effects of climate change on lake ecosystems.

1. Introduction

Freshwater lakes provide essential ecological services such as water supplies, recreation, and biodiversity (Kraemer et al., 2021). However, anthropogenic eutrophication and subsequent harmful algal blooms occurrence have impaired these services (Backer et al., 2015; Brookes & Carey, 2011; Conley et al., 2009; Paerl et al., 2016). Reducing external nutrient loads is a principal strategy to control eutrophication and algal blooms (Abell et al., 2022; Linden et al., 2004). Apart from external nutrient input, internal phosphorus recycling can also influence in-lake phosphorus availability and shape algal blooms dynamics in shallow eutrophic lakes (Qin et al., 2023; Søndergaard et al., 2013). Furthermore, dramatic fluctuations in algal blooms may occur more frequently in a changing climate (Christensen et al., 2006; Istvánovics et al., 2022). Thus, there is a great need to better understand the internal and external driving mechanisms behind algal growth and proliferation.

Nutrients and meteorological conditions are important factors influencing algal biomass and cell buoyancy which lead to blooms (Baker et al., 2000; Brookes et al., 2000; Huisman et al., 2018). Following external nutrient input into the lake, a sequence of biogeochemical processes unfold, including uptake by algae, decomposition and mineralization of detrital phytoplankton, sedimentation, release from sediment, etc (Cole & Likens, 1979; Søndergaard et al., 2013). In these internal nutrient cycling processes, there are positive algae-nutrients feedback loops (Meerhoff et al., 2022; Qin, 2020). Specially, under favorable meteorological conditions, intense algal blooms greatly enhance the quantity and activity of heterotrophic bacteria community, which accelerate the decomposition and mineralization of algal detritus which make nutrients bioavailable (Eiler & Bertilsson, 2004; Grossart et al., 2006; Tang et al., 2010). Degradation of algal detritus can also stimulate nutrients release from sediment through changing the dissolved oxygen further accelerating nutrients cycling (Kang, Zhu, Zhu, et al., 2023; Qin et al., 2023). These feedbacks, in turn, increase blooms magnitude and prolong bloom duration through increasing "additional" nutrient inputs.

The management of phytoplankton is hindered by the large variability in inter- and intra-annual variability of phytoplankton population and identifying the root cause of this variability (Linden et al., 2004). The aim of this

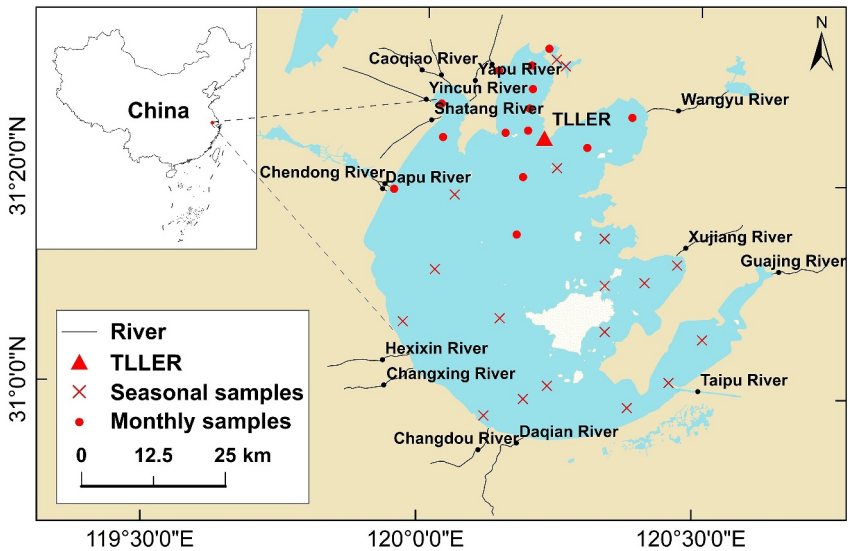

Figure 1. Location of Lake Taihu. Black circles are the main rivers connected to the lake. Red circles are for monthly sampling sites. Red cross signs are for seasonally sampling sites. Red triangle indicates the location of The Taihu Laboratory for Lake Ecosystem Research (TLLER).

study is to assess how water temperature, incident light availability, total suspended solids and nutrient loading affect the phytoplankton communities.

Lake Taihu, the third largest eutrophic freshwater lake in China, is situated in an alluvial plain of Yangtze River. After the severe drinking water crisis in 2007 in Wuxi, the governments initiated many restoration measures to improve water quality (Qin, 2020). The external inputs of total nitrogen and total phosphorus from surrounding rivers start to decline, but remain at high levels (Figure S1 in Supporting Information S1). Meanwhile, algal biomass has undergone remarkable changes in recent years and doesn't respond in a predictable way to the variations in external loading. The algal biomass was considerably higher during 2016–2020 compared to the preceding period from 2008 to 2015. However, following 2020, there has been a notable decline in algal blooms intensity. Wu et al. (2022) identified that the reduced ammonia and nitrate concentrations that resulted from the decreased nutrient load and concentrated rainfall in July–August 2021, significantly reduced the intensity of cyanobacterial blooms. Kang, Zhu, Zou, et al. (2023) highlighted that low external phosphorus supply due to extreme drought led to the observed decrease of algal biomass in 2022. In addition to external loading, the internal phosphorus cycling can also influence in-lake phosphorus availability, and support algal growth (Søndergaard et al., 2013).

The shift from higher algal biomass during 2016–2020 to lower algal biomass during 2021–2023 in Lake Taihu presents an opportunity to explore what mechanisms are driving this shift in algal biomass. We explore this by employing a process-based model simulating how the phytoplankton respond to changes in water temperature, incident light availability, total suspended solids and nutrients during the high-algae period (2016–2020) and the low-algae period (2021–2023).

2. Materials and Methods

2.1. Study Site

Lake Taihu (30°55′40″–31°32′52″N, 119°52′32″–120°36′10″E) is a shallow eutrophic freshwater lake located in the Yangtze River Delta region, China (Figure 1). The lake has a catchment area of 36,500 km^2, a surface area of 2,338 km^2, and a volume of 4.4×10^9 m^3. The mean and maximum depth are 1.9 and 3 m, respectively. Annual freshwater input to the lake averages 8.8×10^9 m^3, and the average water retention time is approximately 180 days (Xu et al., 2015).

The Taihu basin has a complicated river network, with 117 rivers or channels connecting to the lake (Xu et al., 2015). The main inflow rivers, such as Chendonggang, Yincungang and Xitiaoxi, originate from the

southwestern and western watersheds. The primary outflow is through the Taipu River in the eastern watershed. However, the nutrients from the surrounding watersheds are mainly from the northwestern basin and transported to the northern and northwest parts of the lake. The Taihu Basin is located in the East Asian monsoon region, characterized by humid, hot conditions with a prevailing southeast wind in summer (Qin et al., 2021). Algal blooms often occur and persist in the northern or northwestern regions of the lake. The northern Lake Taihu is the focus area of investigation in this study.

2.2. Data Collection

2.2.1. Water Quality and Biological Data

Fourteen sites were monitored monthly and 18 sites were monitored seasonally (February, May, August, and November) from 2005 by The Taihu Laboratory for Lake Ecosystem Research (TLLER). At each site, samples were collected at 0.5 m below the surface, middle of the water column, and 0.5 m above the bottom. The water samples were mixed to represent an integrated water column sample. The water quality and biological indicators can be got after analyzing the water samples. Detailed analytical methods for water quality and biological indicators can be found in Text S1 in Supporting Information S1 and Zhu et al. (2018). The water quality and biological indicators used in this study included ammonium (NH_4^-), nitrate (NO_3^-), nitrite (NO_2^-), phosphate (PO_4^{3-}), and total suspended solids (TSS) from 2016 to 2023. The Chlorophyll a (Chla) and total phosphorus (TP) data was collected from 2005 to 2023. These data are available at http://thl.cern.ac.cn/meta/metaData.

Annual riverine loadings of total nitrogen (TN) and TP from 2005 to 2023 were obtained from *The health status report of Taihu Lake* (https://www.tba.gov.cn/). In addition, a total of 16 main rivers connected to Lake Taihu were monitored monthly from 2016 to 2023. Among the 16 rivers, 12 rivers are inflows while the remaining are outflows. According to the *The health status report of Taihu Lake*, the monitored rivers by TLLER contribute a large proportion of the total inflow into Lake Taihu. The monitored water quality parameters of connected rivers used in this study involved TP and PO_4^{3-}.

2.2.2. Meteorological and Hydrological Data

Water temperature (WT) and water level (WL) were monitored at 8:00, 14:00 and 20:00 every day at the end of pier in the TLLER. WT was measured at 0.5 m below the surface. Daily incident photosynthetically active radiation (PAR), wind speed (WS), and rainfall (RF) were obtained by automatic meteorological station from the TLLER (http://thl.cern.ac.cn/meta/metaData).

2.3. Trend Analysis

The Chla, TSS, DIN (dissolved inorganic nitrogen, the sum of NH_4^-, NO_3^-, and NO_2^-) and PO_4^{3-} concentrations at 14 sampling sites were area-averaged based on the Thiessen polygon method to obtain mean values in the northern Lake Taihu. The seasonal mean WT, WS, PAR, RF, WL, TSS, DIN, and PO_4^{3-} were calculated by averaging the monthly or daily monitoring. The non-parametric Mann-Kendall test was conducted to determine whether significant positive or negative temporal trends existed in these variables at seasonal scale from 2016 to 2023 ($P < 0.05$). Detailed descriptions of the Mann-Kendall test can be found in reference (Kendall, 1975; Mann, 1945).

2.4. The Analysis of Internal Load

The OECD eutrophication model can be used to determine whether internal phosphorus is released into the water column to support the growth of additional algae. The model considers that the in-lake TP concentration is mainly determined by external loading and assumes the internal load is zero on an annual scale (Janus & Vollenweider, 1981). The theoretical in-lake TP concentration is calculated as (Janus & Vollenweider, 1981):

$$P = \frac{l}{q} \cdot \frac{1}{1+\sqrt{\tau}} \tag{1}$$

where l is areal-specific annual phosphorus load ($g \cdot m^{-2} \cdot year^{-1}$), q indicates hydraulic load ($m \cdot year^{-1}$), and τ is the theoretical hydraulic residence time (year).

There exists a significant positive correlation between TP concentration and algal biomass (indicated by Chla) in P-limited lakes. When the calculated theoretical phosphorus concentration is plotted against Chla, it is found that the same theoretical phosphorus concentration might correspond to different Chla concentration. This phenomenon may be attributed to the influence of internal load. Taking the years with the lowest Chla as the baseline, algal growth during these years is sustained by external phosphorus load alongside zero or lower internal phosphorus release. When Chla exceeds the basal level, we can assume that the corresponding year has a higher internal load (Istvánovics et al., 2022). When Chla falls the basal level, it indicates the internal TP load is mainly deposited during the corresponding year. The released or deposited amount of internal TP load can be estimated from the difference between the actual and the basal Chla according to the relationship between the basal Chla and TP values. In this study, the average Chla values between May and August due to the seasonal sampling frequency in the entire Lake Taihu were used to indicate algal biomass (corresponding to the period of algal blooms occurrence in Lake Taihu).

2.5. Quantitative Underlying Mechanism on Algal Biomass Variation

2.5.1. Model Structure

A zero-dimensional process-based model is designed for simulating temporal variation of Chla and PO_4^{3-} concentration. Due to the dominant role of cyanobacteria (mainly Microcystis) in the northern Lake Taihu (Text S2 and Figure S2 in Supporting Information S1), the growth characteristics of cyanobacteria (mainly Microcystis) were mainly considered.

1. Chla simulation module

The module for simulating Chla primarily encompasses processes of algal photosynthesis, respiration, excretion, mortality, and grazing (Bowie et al., 1985; Hipsey et al., 2011).

$$\frac{\partial A}{\partial t} = \left(\mu_g - l_r - l_p - l_m - G\right) \cdot A \tag{2}$$

where μ_g is the algal photosynthetic rate (day^{-1}), l_r is the respiration rate (day^{-1}), l_p is the excretion rate (day^{-1}), l_m is the mortality rate (day^{-1}), and G is the algal loss grazed by zooplankton (day^{-1}). The specific functions of these terms can be seen in Text S3 in Supporting Information S1.

2. Phosphate simulation module

Phosphate concentration is modeled as a function of inflow phosphate input, outflow phosphate output, uptake by algae, decomposition and mineralization of labile organic matter (mainly from algal colonies), zooplankton-mediated recycling, release from sediment, and sedimentation of phosphate (Olson & Jones, 2022; Z.-X. Zhou et al., 2022):

$$\frac{\partial P}{\partial t} = P_{\text{in}} - P_{\text{out}} - \mu_g \cdot A \cdot C_p + L \cdot A \cdot C_p + G \cdot A \cdot \text{rec} + P_{\text{re}} - v \times P \tag{3}$$

where P_{in} is the phosphate inflow ($mg{\cdot}L^{-1}{\cdot}day^{-1}$), P_{out} is the phosphate outflow ($mg{\cdot}L^{-1}{\cdot}day^{-1}$), C_p is the ratio of Chla to Phosphorus (mg·P/(mg·Chla)), *rec* is the proportion of grazed phosphate (dimensionless), P_{re} is the phosphate release from the sediment ($mg{\cdot}L^{-1}\ day^{-1}$), and v is the sedimentation rate of phosphate adsorbed by particulate matter (day^{-1}).

We considered phosphate releasing from sediment as a function of the gradient between sediment and water column, the dissolved oxygen depletion coefficient and WS. Due to limited available data, we assumed the phosphate concentration in the interstitial water of sediment had monthly variations but was constant on a yearly scale. The monthly phosphate values in the interstitial water of sediment were adopted from S. Ding et al. (2018). The dissolved oxygen depletion coefficient was referenced to Charlton (1980) and Genkai-Kato and Carpenter (2005). When strong winds and waves occur, the bottom sediments undergo a resuspension process, carrying nutrients into the water column. The nutrients released from resuspension are primarily in particulate forms (Y. Ding et al., 2011). Therefore, it was assumed that the phosphate released from the sediment during strong waves was zero.

Table 1
Scenarios Design for Identifying Key Drivers of the Phytoplankton Biomass Dynamics

Scenario design	Model input variable				Model input/output variable	Model output variable
	WT (°C)	PAR (mol/m^2/d)	TSS (mg/L)	DIN (mg/L)	PO_4^{3-} (mg/L)	
Control	Stage II	Stage II	Stage II	Stage II	Model output variable	Chla, PO_4^{3-}
S1	Stage I	Stage II	Stage II	Stage II	Using simulated PO_4^{3-} under the Control experiment as model input variable	Chla
S2	Stage II	Stage I	Stage II	Stage II	Using simulated PO_4^{3-} under the Control experiment as model input variable	Chla
S3	Stage II	Stage II	Stage I	Stage II	Using simulated PO_4^{3-} under the Control experiment as model input variable	Chla
S4	Stage II	Stage II	Stage II	Stage I	Using simulated PO_4^{3-} under the Control experiment as model input variable	Chla
S5	Stage I	Stage II	Stage II	Stage II	Model output variable	Chla, PO_4^{3-}
S6	Stage II	Stage I	Stage II	Stage II	Model output variable	Chla, PO_4^{3-}
S7	Stage II	Stage II	Stage I	Stage II	Model output variable	Chla, PO_4^{3-}
S8	Stage II	Stage II	Stage II	Stage I	Model output variable	Chla, PO_4^{3-}

Note. Stage I is the average state of 2016–2020. Stage II is the average state of 2021–2023.

$$\begin{cases} P_{\mathrm{re}} = r \cdot (P_s - P) \cdot \left(3.80 \cdot f(A) \cdot \dfrac{D}{50 + D} \cdot k(T) + 0.12\right) & \mathrm{WS} \le \mathrm{WS}_C \\ P_{\mathrm{re}} = 0 & \mathrm{WS} > \mathrm{WS}_C \end{cases} \tag{4}$$

where r is the coefficient of phosphate release from sediment (day^{-1}), P_S is the phosphate concentration in the interstitial water of sediment (mg·L^{-1}), $f(A) = a \cdot A^b/(K_A + a \cdot A^b)$, D is the water depth (m), $k(T) = 2^{(T-4)/10}$, and WS_C is the critical WS causing sediment suspension (m·s^{-1}).

Riverine inputs of phosphorus are the main part of external phosphorus loading (Qin et al., 2021; Williams & King, 2020). The annual riverine phosphorus input is strongly correlated with rainfall in the Taihu watershed basin (Zhai et al., 2020). Thus, the annual TP riverine input load was allocated to each day according to the ratio of daily RF to annual cumulative RF. We calculated the average ratio of PO_4^{3-}-P to TP based on samples collected from 12 inflow rivers, representing the proportion of PO_4^{3-}-P to TP. Thus, we could obtain daily phosphate load input.

The model was calibrated by comparing simulated Chla and PO_4^{3-} concentration with observed values from 2016 to 2020. Subsequently, the model was validated from 2021 to 2023. The correlation coefficient (R) and relative error (RE) were applied to evaluate the performance of the model. Based on the R and RE values, the model performance can be classified into four categories (fair, satisfactory, good, and excellent) (Kong et al., 2023). The detailed threshold values and assessment criteria for Chla and PO_4^{3-} can be seen in Table S1 in Supporting Information S1. The sensitivity analysis could be found in Text S4 and Figure S3 in Supporting Information S1. The main parameters used in the model were summarized in Table S2 in Supporting Information S1.

2.5.2. Model Simulation Experiments

To determine the underlying mechanism driving the shift from the higher algal biomass between 2016 and 2020 to the lower algal biomass between 2021 and 2023, we conducted one Control experiment and two sets of scenario experiments using the dynamic model described above (Table 1). For the convenience of conducting scenario experiments, we defined Stage I as high algal biomass period (2016–2020) and Stage II as low algal biomass period (2021–2023), respectively. The Control experiment ran the model for 365 days and used the original observed data (WT, PAR, TSS, and DIN) in Stage II as model inputs. Except for the Control experiment, the two

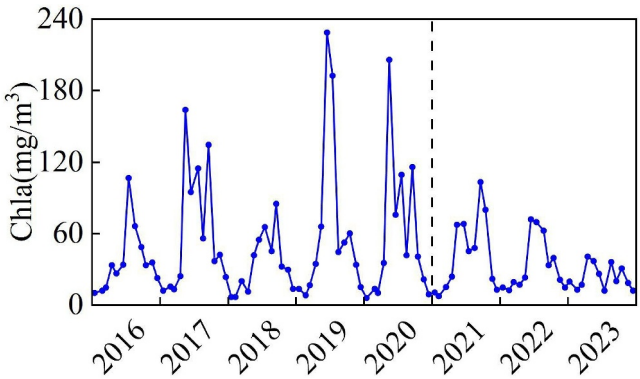

Figure 2. The variation of monthly average Chla concentration in northern Lake Taihu during 2016–2023. The vertical dashed line separates the period of 2016–2020 characterized by higher Chla concentration and the period of 2021–2023 characterized by lower Chla concentration.

sets of scenario experiments included four scenarios with environmental factors changes (i.e., WT, PAR, TSS, and DIN; S1–S4/S5–S8). The difference between S1 and S5 (S2 and S6, S3 and S7, and S4 and S8) was whether considering phosphorus simulation. This was aimed to explore the effects of phosphorus cycling on algal biomass and its contribution to the algal biomass decline during stage II.

3. Results

3.1. The Variations of Algal Biomass and Its Common Influencing Factors

The annual mean Chla concentration showed a non-monotonic pattern during 2016–2023 (Figure 2). The result of Pettitt test showed a tipping point occurred in 2021 ($P = 0.45$, Table S3 in Supporting Information S1). During the period of 2016–2020, the annual mean Chla concentration was 50.8 mg/m^3 with a peak Chla concentration of 229.0 mg/m^3 in June 2019. During 2021–2023, the annual mean Chla concentration was 33.1 mg/m^3. In addition, the highest Chla concentration reached 103.5 mg/m^3 in September 2021, which was lower than the peak Chla concentration during 2016–2020. Annual mean Chla concentration and the intra-year peak Chla concentration in 2023 were both lowest during 2016–2023.

There was seasonal variability of these environmental factors (Figure 3). While WT was increasing, the other factors were decreasing. Furthermore, WS, TSS, DIN, and PO_4^{3-} were decreasing significantly ($P < 0.05$).

Figure 4 indicated the variations of internal phosphorus load during the period of algal blooms occurrence from 2005 to 2023. Internal phosphorus releases were high across 2017, 2019, and 2020. The internal to external TP load ratios were 68.3% in 2017, 56.5% in 2019, and 134.7% in 2020. Internal phosphorus releases were low in 2021 and 2022, in which the internal to external TP load ratios were 19.7% and 23.1%. 2008, 2014, 2015, 2016,

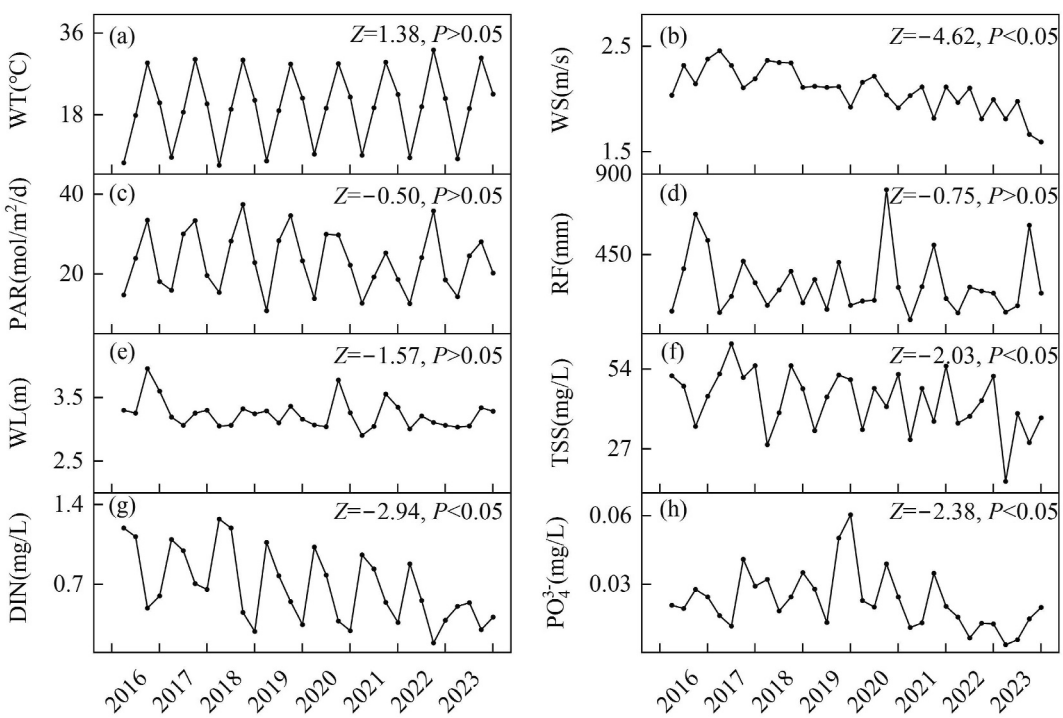

Figure 3. Seasonal trends in (a) WT, (b) WS, (c) PAR, (d) RF, (e) WL, (f) TSS, (g) DIN, and (h) PO_4^{3-}. $Z > 0$ (or $Z < 0$) indicates an increasing (or decreasing) trend. $P < 0.05$ (or $P > 0.05$) indicates the trend is significant (or not significant).

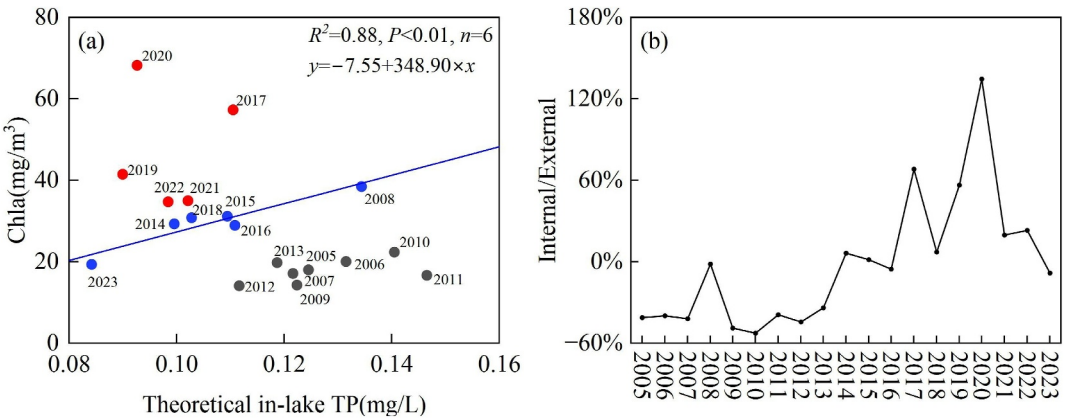

Figure 4. (a) The relationship between mean Chla concentration in May and August and the theoretical in-lake TP concentration, (b) the long-term changes of internal to external TP load ratios. In (a), blue circles indicate years with zero or low internal TP load according to model assumption, red circles indicate years of high internal TP releases, black circles indicate years in which internal loads are mainly deposited, blue line is linear regression for the years with zero or low internal TP load.

2018, and 2023 experienced zero or lower internal phosphorus load. In other years, the internal phosphorus cycling was mainly deposited.

3.2. Results of Model Calibration and Validation

The model reproduced well the inter-annual and monthly variation of Chla and PO_4^{3-} of the observations (Figure 5). According to the model criteria, Chla was simulated with R and RE value of 0.48 and 63.2%, respectively, showing "satisfactory" performance during the calibration period. While in the validation period, the R and RE values were 0.78 and 65.2%, respectively, indicating "satisfactory" performance. The performances for PO_4^{3-} simulation were deemed "satisfactory" for the calibration period (R: 0.48 and RE: 64.7%) and fair for the validation period (R: 0.49 and RE: 87.4%).

3.3. The Variations of Internal Phosphorus Cycling

From 2016 to 2020, the variation of the weekly in-lake PO_4^{3-} concentration was significantly correlated with the amount of internal PO_4^{3-} cycling (Figure 6b, $R^2 = 0.55$, $P < 0.05$). Meanwhile, the correlation coefficient between the variation of weekly in-lake PO_4^{3-} concentration and the inflow PO_4^{3-} was lower (Figure 6a, $R^2 = 0.001$, $P > 0.05$). During the period of 2021–2023, the correlation between the variation of weekly in-lake PO_4^{3-}

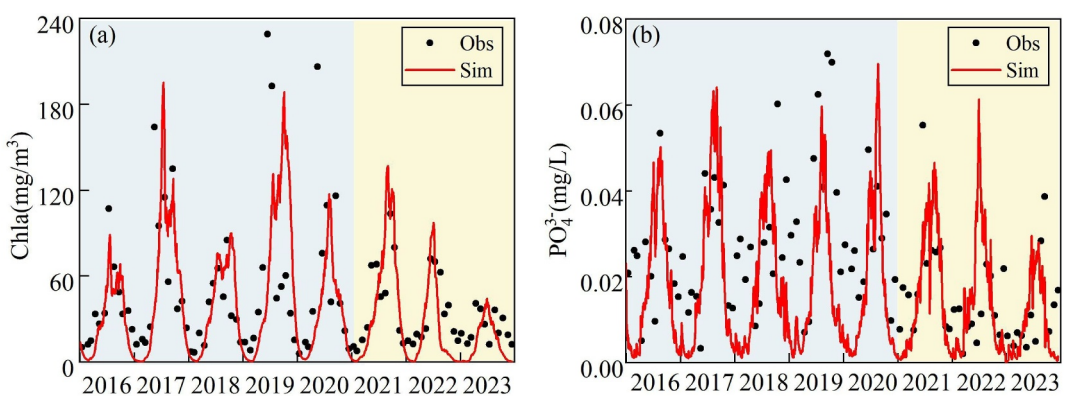

Figure 5. Comparison between observed and simulated (a) Chla and (b) PO_4^{3-} concentrations. The black dots are observed values. The red lines represent simulated values. The blue area indicates the calibration period. The yellow area indicates the validation period.

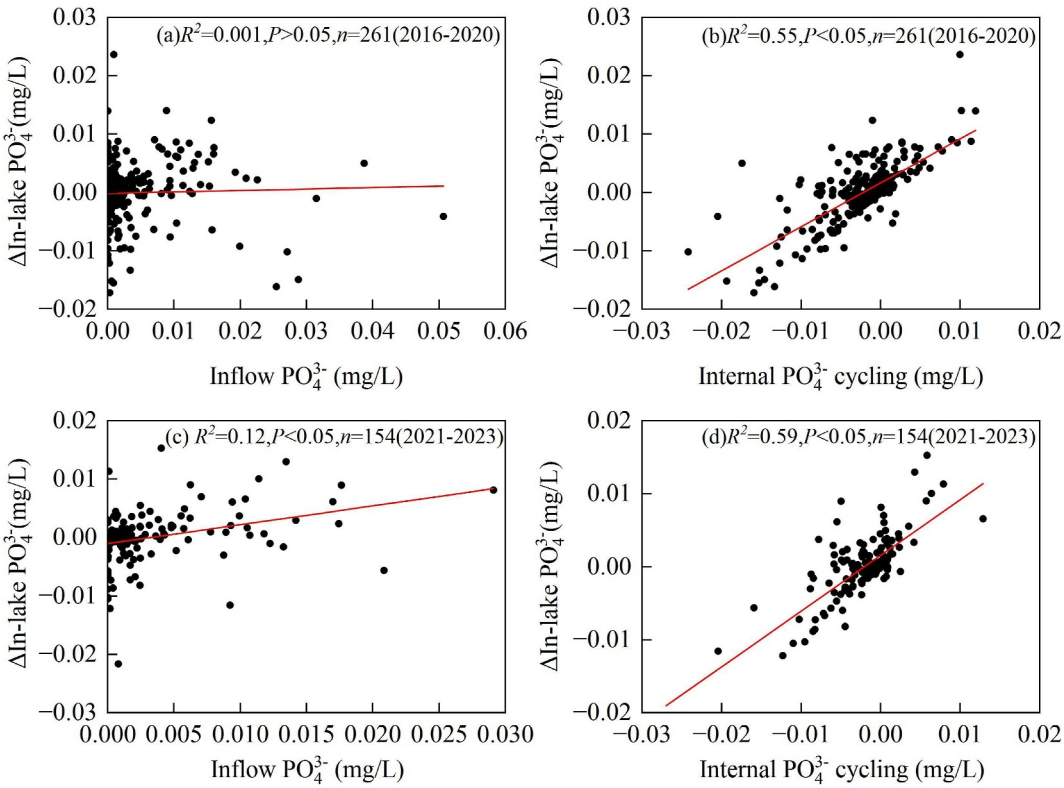

Figure 6. The relationship between (a) the change of in-lake phosphate concentration and the inflow of phosphate on a weekly scale from 2016 to 2020, (b) the change of in-lake phosphate concentration and the amount of internal phosphate cycling on a weekly scale from 2016 to 2020, (c) the change of in-lake phosphate concentration and the inflow of phosphate on a weekly scale from 2021 to 2023, (d) the change of the in-lake phosphate concentration and the amount of internal phosphate cycling on a weekly scale from 2021 to 2023. The red lines are the regression lines.

concentration and the inflow PO_4^{3-} (Figure 6c, $R^2 = 0.12$, $P < 0.05$) was lower than the correlation between the variations of weekly in-lake PO_4^{3-} concentration and the amount of internal PO_4^{3-} cycling (Figure 6d, $R^2 = 0.59$, $P < 0.05$). During 2016–2020, the R^2 of multiple linear regression was 0.72 ($P < 0.05$). The standardized coefficients of internal PO_4^{3-} cycling and inflow PO_4^{3-} were 0.96 and 0.48. During 2021–2023, the R^2 of multiple linear regression was 0.83 ($P < 0.05$). The standardized coefficients of internal PO_4^{3-} cycling and inflow PO_4^{3-} were 0.86 and 0.50.

3.4. Model Scenario Analysis

Among the three meteorological factors (WT, PAR, and TSS), PAR had the greatest impact on the decline of algal biomass in 2021–2023 (Figures 7b and 7d). The phytoplankton community showed a later initiation and shorter duration of blooms, defined as Chla concentration exceeding 40 mg/m^3, under the scenario S2 where PAR changes and the PO_4^{3-} concentration remained the same as the Control experiment when compared to the scenario S6 where PAR changes and the PO_4^{3-} concentration changes based on PAR and phytoplankton abundance. Meanwhile, the mean Chla concentration under S2 and S6 increased 74.5% and 130.4%, respectively, relative to the Control experiment (Figure 7e).

The mean Chla concentration in the scenario S1 of WT alteration and PO_4^{3-} concentration same as the Control experiment exhibited a 8.3% decrease compared to the Control experiment. While under the scenario S5 of WT changes and PO_4^{3-} changes based on WT and phytoplankton abundance, there was a 17.8% decrease in comparison to the Control experiment. The mean Chla concentration in the scenario S3 where TSS changes and PO_4^{3-} same as the Control experiment and the scenario S7 where TSS changes and PO_4^{3-} changes based on TSS and phytoplankton abundance decreased by 24.1% and 29.8%, respectively, compared to the Control experiment.

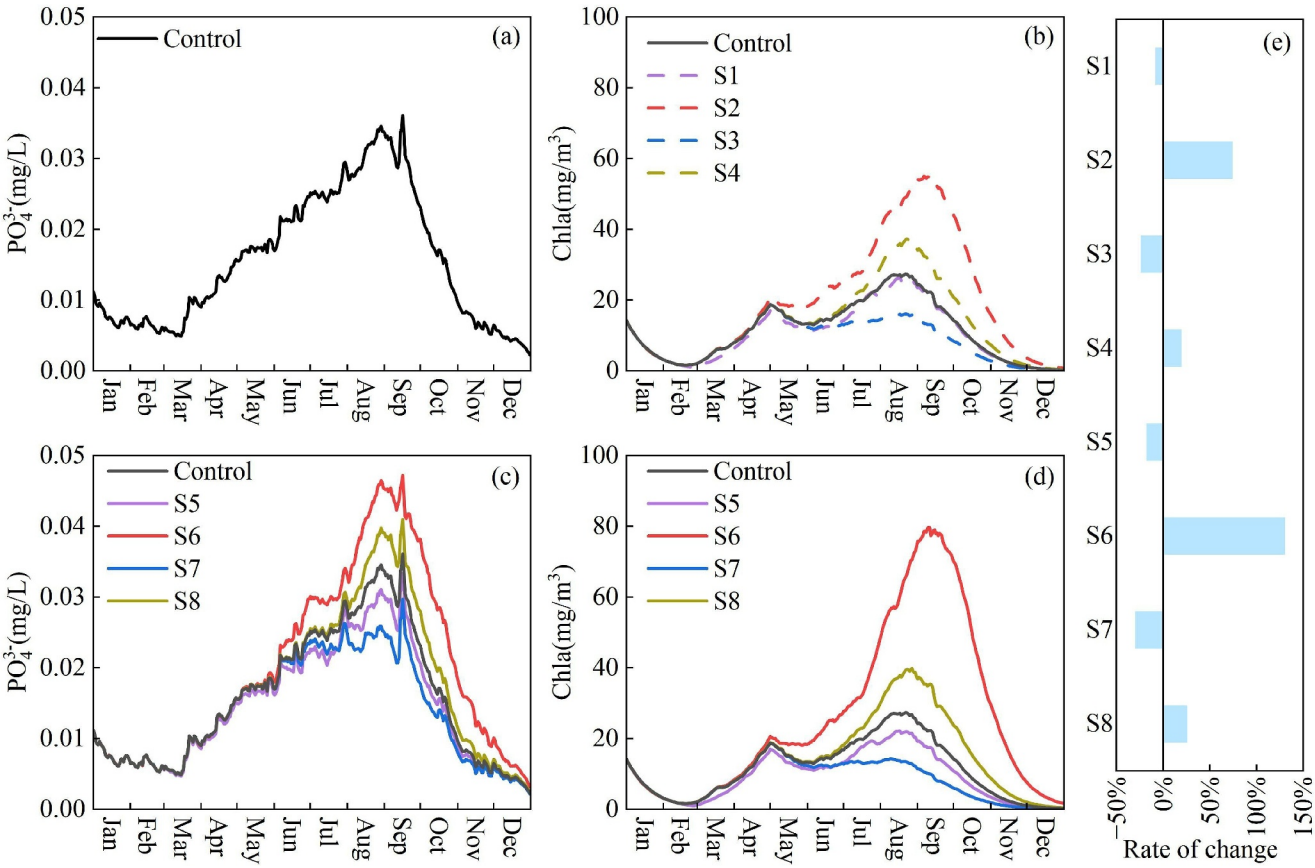

Figure 7. Temporal variations of phosphate and Chla concentrations under the Control experiment and different scenarios (a–d) and the mean change in Chla for different scenarios (e). S1: the scenario where WT changes but PO_4^{3-} same as Control, S2: the scenario where PAR changes but PO_4^{3-} same as Control, S3: the scenario where TSS changes but PO_4^{3-} same as Control, S4: the scenario where DIN changes but PO_4^{3-} same as Control, S5: the scenario where WT changes and PO_4^{3-} changes based on WT and phytoplankton abundance, S6: the scenario where PAR changes and PO_4^{3-} changes based on PAR and phytoplankton abundance, S7: the scenario where TSS changes and PO_4^{3-} changes based on TSS and phytoplankton abundance, S8: the scenario where DIN changes and PO_4^{3-} changes based on DIN and phytoplankton abundance.

Under the scenario S4 where DIN changes and PO_4^{3-} same as the Control experiment and the scenario S8 where DIN changes and PO_4^{3-} changes based on DIN and phytoplankton abundance, the mean Chla concentration were 19.7% and 26.0% greater than the Control experiment, respectively.

4. Discussion

4.1. The Underlying Mechanism Behind Algal Biomass Variation

PAR serves as the primary energy source for photoautotrophic organisms controlling both the rate of growth and the maximum yield when shading occurs (Rastogi et al., 2014). The average monthly incident PAR (except January and December) for 2021–2023 was lower than the average monthly PAR for 2016–2020 (Figure S4 in Supporting Information S1), leading to lower algal photosynthetic rate and lower algal biomass in 2021–2023 (the Control experiment and S2 in Figure 7b). In addition, the phosphate concentration in the water column was also indirectly influenced by the lower PAR. The phosphate concentration under the Control experiment was 21.2% lower than the phosphate concentration under the scenario S6 where PAR changes and the phosphate concentration changes based on PAR and phytoplankton abundance. The lower PAR weakened the positive feedback loop between algae and internal phosphorus cycling. Algae could affect internal nutrient cycling through positive feedback (Cottingham et al., 2015). After the decay of algae, labile organic detritus would be abundant (Cranwell, 1979). The algal detritus can be decomposed by heterotrophic bacteria in the water column, thereby depleting dissolved oxygen and stimulating releasing nutrients from sediment into the water column (Buchan

et al., 2014). When the algal biomass decreases, the released phosphorus from sediment also reduces, in turn, affecting algal growth.

The outcomes of our scenario simulation revealed the decoupling of algal biomass and sediment P release mainly drived the attenuation of cyanobacterial blooms in this large shallow and eutrophic system. The simulated Chla concentration under the scenario where PAR changes but PO_4^{3-} same as the Control experiment revealed that not only a lower peak Chla concentration but also a shorter duration of Chla concentration exceeding 40 mg/m^3 compared to the scenario where PAR changes and PO_4^{3-} changes based on PAR and phytoplankton abundance. This mechanism also partly explained why phosphate concentration in the water column declined in the period of 2021–2023. In low algal biomass period (2021–2023), there was zero or low internal load in 2021, 2022 and 2023 (Figure 4), which also illustrated the weakened algae-phosphorus feedback loop. In contrast to 2021–2023, the positive feedback loop was strengthened in 2016–2020 induced by other meteorological factors. Previous findings in Lake Taihu also demonstrate that severe algal blooms in 2017 can be partly attributed to intense internal nutrient cycling (Pan et al., 2024; Qin et al., 2021; Xu et al., 2021).

During the low algal biomass period (i.e., 2021–2023), the role played by the internal phosphorus cycling could also be emphasized by the small difference between the results of the scenario experiment in which the mean external load during 2021–2023 was replaced with the mean external load during 2016–2020 and the results of the Control experiment (Figure S5 in Supporting Information S1). During the high algal biomass period (i.e., 2016–2020), the changes in in-lake phosphate concentration depended more on the amount of internal phosphate cycling, not on the external input (Figures 6a and 6b). This result further validates the conclusion that significant fluctuations in the internal phosphorus cycling can profoundly influence in-lake phosphorus concentration in eutrophic lakes (Doan et al., 2018; Wang et al., 2019).

During winter and spring, WT is a key limiting factor influencing algal proliferation in eutrophic lakes through affecting enzyme activity (Deng et al., 2014). There was little difference between the simulated Chla value under the Control experiment, S1, and S5 from January to May (Figures 7b and 7d). This occured due to the mean WT in winter from 2016 to 2023 is 7.5°C–9.4°C which were all above the threshold of cyanobacteria starting to grow (Qin et al., 2021) and relatively little algal biomass in initially. During summer, the mean WT exceeds 29°C in Taihu, suggesting WT isn't the primary limiting factor for algal growth (Lürling et al., 2013). The rapid growth of phytoplankton in summer months requires considerable nutrients. In July, the simulated Chla value under the scenario S1 where WT changes but PO_4^{3-} same as the Control experiment started to be closer to the Control experiment, while the simulated Chla value under the scenario S5 WT changes and PO_4^{3-} changes based on WT and phytoplankton abundance was lower than that under the Control experiment (Figures 7b and 7d). This phenomenon indicated the lower WT during 2016–2020 compared to that during 2021–2023 reduced the amount of nutrients formed by the decomposition and mineralization of phytoplankton and releasing from sediment, further decreased Chla value. This is supported by the conclusion that the high growth rates promoted by high summer temperatures require a high supply of nutrients to support the growth and avoid nutrient limitation (Havens et al., 2001).

On a seasonal scale, WS showed a significantly decreasing trend during the study period. While in 2023, the annual mean WS was 1.8 m/s, which was the lowest mean WS over the period from 2016 to 2023. In the extremely shallow Lake Taihu, WS can significantly influence TSS concentration (Y. Zhou et al., 2018). Therefore, the reduction in TSS concentration caused by decreased WS decreased underwater light attenuation, enhanced algal photosynthesis, and increased algal biomass (the Control experiment, S3, and S6 in Figure 7). The decrease in WS can also enhance water column stability and exacerbate hypoxic condition at the lake bottom, which is conducive for releasing nutrients into overlying water and exacerbation of eutrophication (Ranjbar et al., 2022).

The in situ nutrient addition experiments conducted in Meiliang Bay of Lake Taihu indicate nitrogen and phosphorus co-limitation occurs during summer and autumn (Xu et al., 2015). The significant decrease in DIN concentration reduced algal biomass during 2021–2023 (the Control experiment, S4, and S8 in Figure 7). The significant decrease in nitrogen concentration can be attributed to both a reduction in external nitrogen load and high denitrification (Harrison et al., 2009). In addition, the mean Chla concentration under the scenario S8 that DIN changes and PO_4^{3-} changes based on DIN and phytoplankton abundance was higher than the scenario S4

where DIN changes but PO_4^{3-} same as the Control experiment, which further underscored the effects of positive algae-phosphorus feedback loop.

4.2. Model Uncertainty Analysis

The model developed in our study is a process-based model, which has been calibrated and validated, thus, it can be used to predict future algal blooms trend and it is applicable to other similar lake systems. However, the model built in this study has a number of simplifications that may be improved in the future. We didn't specifically address the conversion process from algal debris to organophosphate to phosphate, instead consider the process of conversion from algal debris to phosphate (Olson & Jones, 2022). This assumption is based on some biochemical processes of the organic matter decomposition associated with microorganism metabolism remain unclear. The biochemical process from organophosphate to phosphate can be impacted by meteorological conditions, such as temperature (Malmaeus et al., 2006). Thus, the simplified processes in our study may introduce some uncertainty to the model results, although there is good validation of the model (Figure 5). Due to the overwhelming dominance of cyanobacteria (mainly Microcystis) in the northern Lake Taihu, we mainly considered the growth characteristics of cyanobacteria (Text S2 and Figure S2 in Supporting Information S1). However, the abundance of cyanobacteria decreased in 2023 compared to other years, which might impair model's performance in 2023. In future studies, we would consider the changes in dominant algal species when developing the model.

4.3. Implications

Understanding the complex interplay of multiple stressors and their impacts on algal biomass is important and has been demonstrated to be the primary cause of the shift in lakes from a clear water state to a turbid phytoplankton dominated state (Abell et al., 2022; Ibelings et al., 2007; Kong et al., 2023). After the drinking water crisis in Wuxi in 2007, the government implemented strict lake restoration measures to improve the water quality of Lake Taihu (Qin, 2020). According to *The Health Status Report of Taihu Lake*, the TP load from rivers around Lake Taihu decreased from 2,208 tons in 2008 to 1,400 tons in 2023. The reduction of external TP load into the lake partially decreased phosphorus concentration, yet in-lake phosphorus dynamics were also influenced by internal phosphorus cycling. The continual accumulation of lake sediment from the alluvial plain catchment promotes the release of nutrients from sediment into water column (Ding et al., 2018; Qin et al., 2019). Therefore, we would anticipate a lag between external load reduction and water quality improvement in eutrophic lakes (Carleton & Lee, 2023; Qin, 2020). In changing climate conditions, this lag may be occasional covered because of large variations in meteorological factors. The resilience of eutrophic lakes to increased climate warming predicted under all IPCC scenarios relies on local efforts to reduce nutrient loading and cyanobacterial abundance (Meerhoff et al., 2022). In the context of irreversible climate change, stricter measures for controlling the external load input remain the single most important option to mitigate the effects of climate change on this lake ecosystem (Paerl et al., 2016).

5. Conclusions

Following severe algal blooms during 2016–2020, the algal blooms significantly decreased in the period 2021–2023 in Lake Taihu, China (Figure 2). While earlier studies have explored the impact of physio-chemical factors on the decreased algal biomass (Kang, Zhu, Zou, et al., 2023; Wu et al., 2022), they have not explicitly quantified the influence of internal phosphorus cycling. Through the established process-based model, it is evident that lower PAR and decoupling of the algae-phosphorus interaction induced by lower PAR could be implicated as a major driver of the decline in algal biomass during 2021–2023 in Lake Taihu. This conclusion highlights stricter measures are needed to reduce external loads to weaken this interaction, and further to mitigate the effects of climate change on eutrophic lake ecosystems.

Conflict of Interest

The authors declare no conflicts of interest relevant to this study.

Data Availability Statement

The meteorological and water quality data in Lake Taihu are from the Taihu Laboratory for Lake Ecosystem Research (TLLER), Chinese Academy of Sciences which is available at http://thl.cern.ac.cn/meta/metaData. Annual riverine loadings of total nitrogen (TN) and total phosphorous (TP) were obtained from "The health status report of Taihu Lake" (https://www.tba.gov.cn/). The two websites can be translated into English by the Google Translate plugin in Chrome or the Google Translate site for translation. The full details about the methods can be found in the main text and Supporting Information S1. The data set used in this study is accessible on Zenodo (https://doi.org/10.5281/zenodo.15294905) (Pan & Qin, 2025).

Acknowledgments
This study was funded by National Natural Science Foundation (42220104010, 42001113).

References

Abell, J. M., Ozkundakci, D., Hamilton, D. P., & Reeves, P. (2022). Restoring shallow lakes impaired by eutrophication: Approaches, outcomes, and challenges. *Critical Reviews in Environmental Science and Technology*, *52*(7), 1199–1246. https://doi.org/10.1080/10643389.2020.1854564

Backer, L. C., Manassaram-Baptiste, D., LePrell, R., & Bolton, B. (2015). Cyanobacteria and algae blooms: Review of health and environmental data from the harmful algal bloom-related illness surveillance system (HABISS) 2007–2011. *Toxins*, *7*(4), 1048–1064. https://doi.org/10.3390/toxins7041048

Baker, P. D., Brookes, J. D., Burch, M. D., Maier, H. R., & Ganf, G. G. (2000). Advection, growth and nutrient status of phytoplankton populations in the lower River Murray, South Australia. *Regulated Rivers: Research & Management*, *16*(4), 327–344. https://doi.org/10.1002/1099-1646(200007/08)16:4<327::Aid-rrr576>3.0.Co;2-q

Bowie, G. L., Mills, W. B., Porcella, D. B., Campbell, C. L., Pagenkopf, J. R., Rupp, G. L., et al. (1985). *Rates, constants, and kinetics formulations in surface water quality modeling*. Athens, Ga: O. o. R. a. D. Environmental Research Laboratory, U.S. Environmental Protection Agency. EPA/600/3-85/040.

Brookes, J. D., & Carey, C. C. (2011). Resilience to blooms. *Science*, *334*(6052), 46–47. https://doi.org/10.1126/science.1207349

Brookes, J. D., Ganf, G. G., & Oliver, R. L. (2000). Heterogeneity of cyanobacterial gas-vesicle volume and metabolic activity. *Journal of Plankton Research*, *22*(8), 1579–1589. https://doi.org/10.1093/plankt/22.8.1579

Buchan, A., LeCleir, G. R., Gulvik, C. A., & Gonzalez, J. M. (2014). Master recyclers: Features and functions of bacteria associated with phytoplankton blooms. *Nature Reviews Microbiology*, *12*(10), 686–698. https://doi.org/10.1038/nrmicro3326

Carleton, J. N., & Lee, S. S. (2023). Modeling lake recovery lag times following influent phosphorus loading reduction. *Environmental Modelling & Software*, *162*, 105642. https://doi.org/10.1016/j.envsoft.2023.105642

Charlton, M. N. (1980). Hypolimnion oxygen consumption in lakes: Discussion of productivity and morphometry effects. *Canadian Journal of Fisheries and Aquatic Sciences*, *37*(10), 1531–1539. https://doi.org/10.1139/f80-198

Christensen, M. R., Graham, M. D., Vinebrooke, R. D., Findlay, D. L., Paterson, M. J., & Turner, M. A. (2006). Multiple anthropogenic stressors cause ecological surprises in boreal lakes. *Global Change Biology*, *12*(12), 2316–2322. https://doi.org/10.1111/j.1365-2486.2006.01257.x

Cole, J. J., & Likens, G. E. (1979). Measurements of mineralization of phytoplankton detritus in an oligotrophic lake. *Limnology & Oceanography*, *24*(3), 541–547. https://doi.org/10.4319/lo.1979.24.3.0541

Conley, D. J., Paerl, H. W., Howarth, R. W., Boesch, D. F., Seitzinger, S. P., Havens, K. E., et al. (2009). Controlling eutrophication: Nitrogen and phosphorus. *Science*, *323*(5917), 1014–1015. https://doi.org/10.1126/science.1167755

Cottingham, K. L., Ewing, H. A., Greer, M. L., Carey, C. C., & Weathers, K. C. (2015). Cyanobacteria as biological drivers of lake nitrogen and phosphorus cycling. *Ecosphere*, *6*(1), 1–19. https://doi.org/10.1890/es14-00174.1

Cranwell, P. A. (1979). Decomposition of aquatic biota and sediment formation: Bound lipids in algal detritus and lake sediments. *Freshwater Biology*, *9*(4), 305–313. https://doi.org/10.1111/j.1365-2427.1979.tb01514.x

Deng, J., Qin, B., Paerl, H. W., Zhang, Y., Ma, J., & Chen, Y. (2014). Earlier and warmer springs increase cyanobacterial (Microcystis spp.) blooms in subtropical Lake Taihu, China. *Freshwater Biology*, *59*(5), 1076–1085. https://doi.org/10.1111/fwb.12330

Ding, S., Chen, M., Gong, M., Fan, X., Qin, B., Xu, H., et al. (2018). Internal phosphorus loading from sediments causes seasonal nitrogen limitation for harmful algal blooms. *Science of the Total Environment*, *625*, 872–884. https://doi.org/10.1016/j.scitotenv.2017.12.348

Ding, Y., Zhu, G., Qin, B., Wang, Y., Wu, T., Shen, X., & Hong, D. (2011). Experimental study on the effect of wave disturbances on the phosphorus dynamics in shallow lakes. *Advances in Water Science*, *22*(2), 273–278.

Doan, P. T. K., Watson, S. B., Markovic, S., Liang, A., Guo, J., Mugalingam, S., et al. (2018). Phosphorus retention and internal loading in the Bay of Quinte, Lake Ontario, using diagenetic modelling. *Science of the Total Environment*, *636*, 39–51. https://doi.org/10.1016/j.scitotenv.2018.04.252

Eiler, A., & Bertilsson, S. (2004). Composition of freshwater bacterial communities associated with cyanobacterial blooms in four Swedish lakes. *Environmental Microbiology*, *6*(12), 1228–1243. https://doi.org/10.1111/j.1462-2920.2004.00657.x

Genkai-Kato, M., & Carpenter, S. R. (2005). Eutrophication due to phosphorus recycling in relation to lake morphometry, temperature, and macrophytes. *Ecology*, *86*(1), 210–219. https://doi.org/10.1890/03-0545

Grossart, H.-P., Czub, G., & Simon, M. (2006). Algae-bacteria interactions and their effects on aggregation and organic matter flux in the sea. *Environmental Microbiology*, *8*(6), 1074–1084. https://doi.org/10.1111/j.1462-2920.2006.00999.x

Harrison, J. A., Maranger, R. J., Alexander, R. B., Giblin, A. E., Jacinthe, P.-A., Mayorga, E., et al. (2009). The regional and global significance of nitrogen removal in lakes and reservoirs. *Biogeochemistry*, *93*(1–2), 143–157. https://doi.org/10.1007/s10533-008-9272-x

Havens, K. E., Kukushima, T., Xie, P., Iwakuma, T., James, R. T., Takamura, N., et al. (2001). Nutrient dynamics and the eutrophication of shallow lakes Kasumigaura (Japan), Donghu (PR China), and Okeechobee (USA). *Environmental Pollution*, *111*(2), 263–272. https://doi.org/10.1016/s0269-7491(00)00074-9

Hipsey, M. R., Antenucci, J. P., & Hamilton, D. (2011). *Computational aquatic ecosystem dynamics model: CAEDYM v3*. Centre for Water Research, University of Western Australia.

Huisman, J., Codd, G. A., Paerl, H. W., Ibelings, B. W., Verspagen, J. M. H., & Visser, P. M. (2018). Cyanobacterial blooms. *Nature Reviews Microbiology*, *16*(8), 471–483. https://doi.org/10.1038/s41579-018-0040-1

Ibelings, B. W., Portielje, R., Lammens, E. H. R. R., Noordhuis, R., van den Berg, M. S., Joosse, W., & Meijer, M. L. (2007). Resilience of alternative stable states during the recovery of shallow lakes from eutrophication: Lake Veluwe as a case study. *Ecosystems*, *10*(1), 4–16. https://doi.org/10.1007/s10021-006-9009-4

Istvánovics, V., Honti, M., Torma, P., & Kousal, J. (2022). Record-setting algal bloom in polymictic Lake Balaton (Hungary): A synergistic impact of climate change and (mis)management. *Freshwater Biology*, *67*(6), 1091–1106. https://doi.org/10.1111/fwb.13903

Janus, L. L., & Vollenweider, R. A. (1981). The OECD cooperative programme on eutrophication: Canadian contribution: Summary report. E. Canada.

Kang, L., Zhu, G., Zhu, M., Xu, H., Zou, W., Xiao, M., et al. (2023). Bloom-induced internal release controlling phosphorus dynamics in large shallow eutrophic Lake Taihu, China. *Environmental Research*, *231*, 116251. https://doi.org/10.1016/j.envres.2023.116251

Kang, L., Zhu, G., Zou, W., Zhu, M., Guo, C., Xu, H., et al. (2023). Dynamics and mechanism of cyanobacterial blooms in Lake Taihu reacted extreme drought and warming. *Journal of Lake Sciences*, *35*(6), 1866–1880. https://doi.org/10.18307/2023.0611

Kendall, M. G. (1975). *Rank correlation methods* (4th ed.). Charles Griffin.

Kong, X., Determann, M., Andersen, T. K., Barbosa, C. C., Dadi, T., Janssen, A. B. G., et al. (2023). Synergistic effects of warming and internal nutrient loading interfere with the long-term stability of lake restoration and induce sudden re-eutrophication. *Environmental Science & Technology*, *57*(9), 4003–4013. https://doi.org/10.1021/acs.est.2c07181

Kraemer, B. M., Pilla, R. M., Woolway, R. I., Anneville, O., Ban, S., Colom-Montero, W., et al. (2021). Climate change drives widespread shifts in lake thermal habitat. *Nature Climate Change*, *11*(6), 521–529. https://doi.org/10.1038/s41558-021-01060-3

Linden, L. G., Lewis, D. M., Burch, M. D., & Brookes, J. D. (2004). Interannual variability in rainfall and its impact on nutrient load and phytoplankton in Myponga Reservoir, South Australia. *International Journal of River Basin Management*, *2*(3), 169–179. https://doi.org/10.1080/15715124.2004.9635230

Lürling, M., Eshetu, F., Faassen, E. J., Kosten, S., & Huszar, V. L. M. (2013). Comparison of cyanobacterial and green algal growth rates at different temperatures. *Freshwater Biology*, *58*(3), 552–559. https://doi.org/10.1111/j.1365-2427.2012.02866.x

Malmaeus, J. M., Blenckner, T., Markensten, H., & Persson, I. (2006). Lake phosphorus dynamics and climate warming: A mechanistic model approach. *Ecological Modelling*, *190*(1–2), 1–14. https://doi.org/10.1016/j.ecolmodel.2005.03.017

Mann, H. B. (1945). Nonparametric tests against trend. *Econometrica: Journal of the Econometric Society*, *13*(3), 245–259. https://doi.org/10.2307/1907187

Meerhoff, M., Audet, J., Davidson, T. A., De Meester, L., Hilt, S., Kosten, S., et al. (2022). Feedback between climate change and eutrophication: Revisiting the allied attack concept and how to strike back. *Inland Waters*, *12*(2), 187–204. https://doi.org/10.1080/20442041.2022.2029317

Olson, C. R., & Jones, S. E. (2022). Chlorophyll-total phosphorus relationships emerge from multiscale interactions from algae to catchments. *Limnology and Oceanography Letters*, *7*(6), 483–491. https://doi.org/10.1002/lol2.10281

Paerl, H. W., Gardner, W. S., Havens, K. E., Joyner, A. R., McCarthy, M. J., Newell, S. E., et al. (2016). Mitigating cyanobacterial harmful algal blooms in aquatic ecosystems impacted by climate change and anthropogenic nutrients. *Harmful Algae*, *54*, 213–222. https://doi.org/10.1016/j.hal.2015.09.009

Pan, T., Cui, C., Qin, B., Ding, K., & Zhou, J. (2024). Climate change intensifies algal biomass resurgence in eutrophic Lake Taihu, China. *Science of the Total Environment*, *926*, 171934. https://doi.org/10.1016/j.scitotenv.2024.171934

Pan, T., & Qin, B. (2025). Dataset for the study of algal biomass variation [Dataset]. *Zenodo*. https://doi.org/10.5281/zenodo.15294905

Qin, B. (2020). Shallow lake limnology and control of eutrophication in Lake Taihu. *Journal of Lake Sciences*, *32*(5), 1229–1243. https://doi.org/10.18307/2020.0501

Qin, B., Deng, J., Shi, K., Wang, J., Brookes, J., Zhou, J., et al. (2021). Extreme climate anomalies enhancing cyanobacterial blooms in Eutrophic Lake Taihu, China. *Water Resources Research*, *57*(7). https://doi.org/10.1029/2020wr029371

Qin, B., Paerl, H. W., Brookes, J. D., Liu, J., Jeppesen, E., Zhu, G., et al. (2019). Why Lake Taihu continues to be plagued with cyanobacterial blooms through 10 years (2007–2017) efforts. *Science Bulletin*, *64*(6), 354–356. https://doi.org/10.1016/j.scib.2019.02.008

Qin, B., Zhang, Y., Zhu, G., & Gao, G. (2023). Eutrophication control of large shallow lakes in China. *Science of the Total Environment*, *881*, 163494. https://doi.org/10.1016/j.scitotenv.2023.163494

Ranjbar, M. H., Hamilton, D. P., Etemad-Shahidi, A., & Helfer, F. (2022). Impacts of atmospheric stilling and climate warming on cyanobacterial blooms: An individual-based modelling approach. *Water Research*, *221*, 118814. https://doi.org/10.1016/j.watres.2022.118814

Rastogi, R. P., Sinha, R. P., Moh, S. H., Lee, T. K., Kottuparambil, S., Kim, Y.-J., et al. (2014). Ultraviolet radiation and cyanobacteria. *Journal of Photochemistry and Photobiology B-Biology*, *141*, 154–169. https://doi.org/10.1016/j.jphotobiol.2014.09.020

Søndergaard, M., Bjerring, R., & Jeppesen, E. (2013). Persistent internal phosphorus loading during summer in shallow eutrophic lakes. *Hydrobiologia*, *710*(1), 95–107. https://doi.org/10.1007/s10750-012-1091-3

Tang, X., Gao, G., Chao, J., Wang, X., Zhu, G., & Qin, B. (2010). Dynamics of organic-aggregate-associated bacterial communities and related environmental factors in Lake Taihu, a large eutrophic shallow lake in China. *Limnology & Oceanography*, *55*(2), 469–480. https://doi.org/10.4319/lo.2009.55.2.0469

Wang, M., Xu, X., Wu, Z., Zhang, X., Sun, P., Wen, Y., et al. (2019). Seasonal pattern of nutrient limitation in a eutrophic lake and quantitative analysis of the impacts from internal nutrient cycling. *Environmental Science & Technology*, *53*(23), 13675–13686. https://doi.org/10.1021/acs.est.9b04266

Williams, M. R., & King, K. W. (2020). Changing rainfall patterns over the Western Lake Erie Basin (1975–2017): Effects on tributary discharge and phosphorus load. *Water Resources Research*, *56*(3). https://doi.org/10.1029/2019wr025985

Wu, D., Chen, F., Hu, J., Ji, G., Shi, Y., & Shen, A. (2022). The declining cyanobacterial blooms in Lake Taihu (China) in 2021: The interplay of nutrients and meteorological determinants. *Ecological Indicators*, *145*, 109590. https://doi.org/10.1016/j.ecolind.2022.109590

Xu, H., McCarthy, M. J., Paerl, H. W., Brookes, J. D., Zhu, G., Hall, N. S., et al. (2021). Contributions of external nutrient loading and internal cycling to cyanobacterial bloom dynamics in Lake Taihu, China: Implications for nutrient management. *Limnology & Oceanography*, *66*(4), 1492–1509. https://doi.org/10.1002/lno.11700

Xu, H., Paerl, H. W., Qin, B., Zhu, G., Hall, N. S., & Wu, Y. (2015). Determining critical nutrient thresholds needed to control harmful cyanobacterial blooms in Eutrophic Lake Taihu, China. *Environmental Science & Technology*, *49*(2), 1051–1059. https://doi.org/10.1021/es503744q

Zhai, S., Zhou, Y., Cheng, Y., Cai, J., & Hu, Y. (2020). Calculation of total phosphorus loads from rivers around Lake Taihu and analysis of total phosphorus fluctuation in the lake in 2015–2016. *Journal of Lake Sciences*, *32*(1), 48–57. https://doi.org/10.18307/2020.0105

Zhou, Y., Liu, J. E., Xu, X., Qi, C., Wu, X., Lin, H., & Shi, K. (2018). Response of suspended solids and dissolved nutrients in littoral zone of Lake Taihu under wind-wave disturbances. *Journal of Lake Sciences*, *30*(4), 948–956. https://doi.org/10.18307/2018.0408

Zhou, Z.-X., Yu, R.-C., & Zhou, M. J. (2022). Evolution of harmful algal blooms in the East China Sea under eutrophication and warming scenarios. *Water Research*, *221*, 118807. https://doi.org/10.1016/j.watres.2022.118807

Zhu, G., Qin, B., Zhang, Y., Xu, H., Zhu, M., Yang, H., et al. (2018). Variation and driving factors of nutrients and chlorophyll-a concentrations in northern region of Lake Taihu, China, 2005–2017. *Journal of Lake Sciences*, *30*(2), 279–295. https://doi.org/10.18307/2018.0201

References From the Supporting Information

Blauw, A. N., Los, H. F. J., Bokhorst, M., & Erftemeijer, P. L. A. (2009). GEM: A generic ecological model for estuaries and coastal waters. *Hydrobiologia*, *618*(1), 175–198. https://doi.org/10.1007/s10750-008-9575-x

Cao, H.-S., Tao, Y., Kong, F.-X., & Yang, Z. (2008). Relationship between temperature and cyanobacterial recruitment from sediments in laboratory and field studies. *Journal of Freshwater Ecology*, *23*(3), 405–412. https://doi.org/10.1080/02705060.2008.9664217

Chapra, S. C., Boehlert, B., Fant, C., Bierman, V. J., Jr., Henderson, J., Mills, D., et al. (2017). Climate change impacts on harmful algal blooms in US freshwaters: A screening-level assessment. *Environmental Science & Technology*, *51*(16), 8933–8943. https://doi.org/10.1021/acs.est.7b01498

Cho, E., Arhonditsis, G. B., Khim, J., Chung, S., & Heo, T.-Y. (2016). Modeling metal-sediment interaction processes: Parameter sensitivity assessment and uncertainty analysis. *Environmental Modelling & Software*, *80*, 159–174. https://doi.org/10.1016/j.envsoft.2016.02.026

Gao, J., Zhu, J., & Dong, W. (2019). Influence mechanism of light on common algae and its application. *Environmental Engineering*, *37*(5), 111–116. https://doi.org/10.13205/j.hjgc.201905021

Gulati, R. D., & DeMott, W. R. (1997). The role of food quality for zooplankton: Remarks on the state-of-the-art, perspectives and priorities. *Freshwater Biology*, *38*(3), 753–768. https://doi.org/10.1046/j.1365-2427.1997.00275.x

Hamilton, D. P., & Schladow, S. G. (1997). Prediction of water quality in lakes and reservoirs. 1. Model description. *Ecological Modelling*, *96*(1–3), 91–110. https://doi.org/10.1016/s0304-3800(96)00062-2

Huang, J., Gao, J., & Hoermann, G. (2012). Hydrodynamic-phytoplankton model for short-term forecasts of phytoplankton in Lake Taihu, China. *Limnologica*, *42*(1), 7–18. https://doi.org/10.1016/j.limno.2011.06.003

Ji, Z.-G. (2017). *Hydrodynamics and water quality: Modeling rivers, lakes, and Estuaries* (2nd ed.). John Wiley and Sons, Inc. https://doi.org/10.1002/9781119371946

Jiang, L., Li, Y., Zhang, S., Wang, W., Weng, S., Du, W., & Wang, J. (2018). Parameter sensitivity analysis of algal model in large shallow lakes. *Journal of Lake Sciences*, *30*(3), 693–700. https://doi.org/10.18307/2018.0311

Knightes, C. D., Ambrose, R. B., Jr., Avant, B., Han, Y., Acrey, B., Bouchard, D. C., et al. (2019). Modeling framework for simulating concentrations of solute chemicals, nanoparticles, and solids in surface waters and sediments: WASP8 advanced toxicant module. *Environmental Modelling & Software*, *111*, 444–458. https://doi.org/10.1016/j.envsoft.2018.10.012

Luo, X., & Li, X. (2018). Using the EFDC model to evaluate the risks of eutrophication in an urban constructed pond from different water supply strategies. *Ecological Modelling*, *372*, 1–11. https://doi.org/10.1016/j.ecolmodel.2018.01.020

Paerl, H. W., & Otten, T. G. (2013). Harmful cyanobacterial blooms: Causes, consequences, and controls. *Microbial Ecology*, *65*(4), 995–1010. https://doi.org/10.1007/s00248-012-0159-y

Reynolds, C. S., Irish, A. E., & Elliott, J. A. (2001). The ecological basis for simulating phytoplankton responses to environmental change (PROTECH). *Ecological Modelling*, *140*(3), 271–291. https://doi.org/10.1016/s0304-3800(01)00330-1

Steele, J. H. (1962). Environmental control of photosynthesis in the sea. *Limnology & Oceanography*, *7*(2), 137–150. https://doi.org/10.4319/lo.1962.7.2.0137

Tett, P., Cottrell, J. C., Trew, D. O., & Wood, B. J. B. (1975). Phosphorus quota and the chlorophyll: Carbon ratio in marine phytoplankton. *Limnology & Oceanography*, *20*(4), 587–603. https://doi.org/10.4319/lo.1975.20.4.0587

Tong, Y., Xu, X., Qi, M., Sun, J., Zhang, Y., Zhang, W., et al. (2021). Lake warming intensifies the seasonal pattern of internal nutrient cycling in the eutrophic lake and potential impacts on algal blooms. *Water Research*, *188*, 116570. https://doi.org/10.1016/j.watres.2020.116570

Verspagen, J. M. H., Snelder, E., Visser, P. M., Jöhnk, K. D., Ibelings, B. W., Mur, L. R., & Huisman, J. (2005). Benthic–pelagic coupling in the population dynamics of the harmful cyanobacterium *Microcystis*. *Freshwater Biology*, *50*(5), 854–867. https://doi.org/10.1111/j.1365-2427.2005.01368.x

Wang, C., Yu, Y., Sun, Y., Li, H., Kong, F., Zhang, M., et al. (2013). The discussion of the early forecasting of cyanobacteria bloom in the Lake Taihu based on ELCOM-CAEDYM model. *China Environmental Science*, *33*(3), 491–502.

Zhang, C., & Fu, T. (2023). Recalibration of a three-dimensional water quality model with a newly developed autocalibration toolkit (EFDC-ACT v1.0.0): How much improvement will be achieved with a wider hydrological variability? *Geoscientific Model Development*, *16*(14), 4315–4329. https://doi.org/10.5194/gmd-16-4315-2023

Zhang, Y., Qin, B., Chen, W., & Yang, D. (2004). Regression analysis of beam attenuation coefficient under water in Lake Taihu. *Oceanologia et Limnologia Sinica*, *35*(3), 209–213. https://doi.org/10.3321/j.issn:0029-814X.2004.03.003